Available online at www.sciencedirect.com
ScienceDirect
Trans. Nonferrous Met. Soc. China 29(2019) 1696−1704
Transactions of Nonferrous Metals Society of China
www.tnmsc.cn

Effects of Ag contents in Sn–*x*Ag lead-free solders on microstructure, corrosion behavior and interfacial reaction with Cu substrate

Phacharaphon TUNTHAWIROON, Kannachai KANLAYASIRI

Department of Industrial Engineering, Faculty of Engineering,
King Mongkut's Institute of Technology Ladkrabang, Bangkok 10520, Thailand

Received 12 November 2018; accepted 25 April 2019

Abstract: The effects of Ag on the microstructure and corrosion behavior of pre-soldering Sn−*x*Ag lead-free solders, and on the formation of intermetallic layer of the solders with Cu substrate were investigated. The Ag contents (*x*) were 0, 3.0, 3.5, 4.0, and 5.0 wt.%. The Ag content played a role in the morphology of Ag_3Sn phase in the solders. The microstructure analysis showed that the *β*-Sn phase was surrounded by eutectic networks in the 3.0Ag and 3.5Ag solders and large plate-like Ag_3Sn formed in the 4.0Ag and 5.0Ag solders. Nonetheless, the Ag content slightly impacted the corrosion behavior of the as-cast solders as characterized using potentiodynamic polarization test. After soldering, only a single layer of a Cu_6Sn_5 intermetallic compound formed at the Sn–*x*Ag/Cu interface. By comparison, the Cu_6Sn_5 intermetallic layer of the Ag-doped solders was thinner than that of the 0Ag solder. The fine Ag_3Sn particles in the eutectic networks precipitating in the 3.0Ag and 3.5Ag solders effectively hindered the growth of Cu_6Sn_5 grains compared to large plate-like Ag_3Sn in the 4.0 and 5.0Ag solders.

Key words: Sn−Ag lead-free solders; microstructure; Ag_3Sn intermetallic phase; corrosion behavior; Cu_6Sn_5 intermetallic layer; wettability

1 Introduction

The European Union's Restriction of Hazardous Substances (RoHS) directive restricts the use of hazardous substances in electronics goods and several other products [1]. Of particular interest is lead (Pb) which tops the list of the banned hazardous substances, despite the low cost, low melting temperature (180 °C), and good wettability [2,3]. The prohibition of lead necessitates electronics packaging manufacturers to explore alternative lead-free solders.

The traditional lead-containing solders are being replaced by the binary and ternary lead-free Sn-based solder systems. The binary solder system is realized by incorporating alloying elements (e.g., Zn, Bi, In, Cu, Ag) into the Sn-based solder to manipulate the solder characteristics for diverse applications [1,2,4−7]. Nevertheless, the addition of alloying elements induces the formation of intermetallic phases and alters the mechanical properties and melting temperatures of the solder.

Specifically, compared to the Sn−Pb system, the Sn−Bi solder with eutectic composition achieves a lower melting temperature but is susceptible to crack due to the inherent brittle nature of Bi [1]. The Sn−Cu solder system exhibits good ductility and conductivity but suffers from high melting temperatures (227 °C for eutectic composition). The Sn−Ag solder possesses good conductivity and good resistance to creep and thermal fatigue, but is costly and has a high melting temperature (221 °C) [8]. Meanwhile, the ternary Sn−Ag−Cu solder system is commonly used due to lower melting temperatures (217−221 °C) as a result of near eutectic composition (i.e. Sn−3.0Ag−0.5Cu). The Sn−Ag−Cu solder system also exhibits good electrical conductivity and high solder joint strength compared with the Sn−Pb, Sn−Cu, and Sn−Ag solder systems [4,9]. However, the ternary system is predisposed to the formation of multiple intermetallic phases and layers during the soldering process, adversely altering the mechanical properties of solder joints [4,7].

The corrosion behavior of the solder also plays a part in the durability and reliability of solder joints [10].

Corresponding author: Phacharaphon TUNTHAWIROON; E-mail: phacharaphon.tu@kmitl.ac.th
DOI: 10.1016/S1003-6326(19)65076-4

By and large, the solder should be resistant to a corrosive environment, such as moisture and heat [11]. Existing research on the corrosion behavior of solders focused mainly on the solders with near eutectic composition, including Sn−0.7Cu, Sn−3.5Ag, and SAC305 solders [10−14]. Moreover, alloying elements (e.g., Zn, Ce, Al, Ag, In) were incorporated into the solder to improve the corrosion resistance [2,3,13,15,16]. Nonetheless, alloying elements contributed to complex microstructures and subsequent lower mechanical properties. Like the ternary solder system, high contents of alloying elements in the Sn-based solders induced several brittle intermetallic phases that decrease the strength and ductility of both pre-soldering solders and the solder joints [9,17−19].

Based on the previous reports [20,21], the Sn−Ag solder system exhibited better corrosion resistance than the lead-based, Sn−Cu, and SAC solders. Furthermore, a fine intermetallic phase of Ag_3Sn was only formed during soldering, which in turn hindered the growth of brittle intermetallic layer of Cu_6Sn_5 [14,22]. Specifically, near eutectic Sn−3.5Ag (wt.%) lead-free solder is commonly used in the electronic industry due to its lowest melting temperature of 221 °C and uniformly distributed fine-eutectic microstructure, compared Sn−Ag solders with the hypoeutectic and hypereutectic composition [5]. However, during the soldering, variation in cooling rates affected the eutectic reaction of Sn−3.5Ag solder, resulting in non-uniformly distributed fine-eutectic microstructure [23,24]. Moreover, there exists limited research on the relationship between the Ag contents and microstructure as well as corrosion behavior in Sn−*x*Ag solder systems. This research thus focuses on the Sn−*x*Ag solder. Specifically, the effects of different Ag contents on the microstructure and corrosion behavior of the Sn−*x*Ag lead-free solders, and the intermetallic layer of the solders with Cu substrate were investigated. The Ag contents (*x*), based on the commercially available Sn−Ag lead-free solders, were varied at 0, 3.0, 3.5, 4.0, and 5.0 wt.%. The low-Ag content (1−2 wt.%) Sn-rich solders were deliberately excluded due to the higher sensitivity to the cooling rate compared with the near-eutectic and high-Ag-rich solders [25].

2 Experimental

In this work, the as-cast Sn−*x*Ag lead-free solders were acquired from Ultracore (Thailand), where *x* is the Ag content at 0 (pure Sn), 3.0, 3.5, 4.0, and 5.0 wt.% (Table 1). Prior to analysis, the solder ingot was sliced into square-shaped thin-sheet specimens of 15 mm× 15 mm×4 mm using a low-speed high-precision cut-off machine (Minitom, Struers). The specimens were ground off by abrasive paper and polished with 1 μm and 0.3 μm alumina suspensions (AP-D suspension, Struers). The polished specimens were then cleaned with ethanol in an ultrasonic cleaner and air-dried.

Table 1 Chemical composition of experimental Sn−*x*Ag solders

Experimental solder	Sn (Ag) content/wt.%
Sn–0Ag	100 (0)
Sn–3.0Ag	97 (3.0)
Sn–3.5Ag	96.5 (3.5)
Sn–4.0Ag	96 (4.0)
Sn–5.0Ag	95 (5.0)

In the microstructure analysis, the sonicated specimens were ion-milled using low-energy Ar ion gun with 6 keV for 5 min (IM4000, Hitachi). The as-cast solder matrix and intermetallic compounds of the experimental solders (0Ag, 3.0Ag, 3.5Ag, 4.0Ag, 5.0Ag solders) were characterized by a scanning electron microscope (SEM; SU3500, Hitachi). The chemical composition of intermetallic compounds was determined by field emission scanning electron microscope (FE-SEM; JSM−760F, JEOL) equipped with energy-dispersive X-ray spectroscopy (EDS).

The corrosion behavior of the experimental solders was determined by potentiodynamic polarization in accordance with the ASTM G 102 standard. Prior to the corrosion experiment, the sonicated specimens were retained for 24 h and then rinsed with ethanol. The polarization test was carried out using three-electrode polarization cell, comprising a working electrode (i.e., Sn−*x*Ag solders), counter electrode (platinum wire), and reference electrode (saturated calomel electrode, SCE). A 3.5 wt.% NaCl solution (500 mL) was used as electrolyte (without reuse). In the experiment, the working electrode was immersed in the NaCl solution for 120 s to realize the open circuit potential (OCP). The potential for corrosion test was varied between −1.2 and 0 V at a rate of 0.033 V/s. The experiments were individually carried out in triplicate. The morphology and chemical composition of corrosion products were subsequently characterized by SEM-EDS.

The interfacial reaction on Cu substrate was determined in accordance with the JIS Z3198-3 standard. The Sn−*x*Ag solders and Cu substrate were 6 mm × 2 mm and 15 mm × 15 mm × 0.5 mm, and the soldering condition was 260 °C for 30 s [26]. The solder wettability and the morphology and thickness of the intermetallic layer between Sn−*x*Ag solder and Cu substrate were then determined.

3 Results and discussion

3.1 Microstructure of as-cast Sn−*x*Ag solders

Figure 1 illustrates the SEM and BSE-SEM microstructures of the 0Ag solder (pure Sn), consisting of large-equiaxed grains of 100 μm on average, with the contrast indicating variation in crystallographic orientation (Fig. 1(b)). Figures 2(a−d) depict the SEM images of as-cast 3.0Ag, 3.5Ag, 4.0Ag, and 5.0Ag solders, respectively. The microstructure analysis revealed *β*-Sn phase (dark color area) and fine lamellar eutectic networks of *β*-Sn and eutectic Ag_3Sn phases (light color area). Specifically, in the 3.0Ag and 3.5Ag solders, the *β*-Sn phase was surrounded by fine lamellar networks (Figs. 2(a, b)), while large plate-like Ag_3Sn phase was formed in the 4.0Ag and 5.0Ag solders (Figs. 2(c, d)).

Based on the phase diagram of Sn−Ag solder system, the solder microstructure is of nearly full eutectic structure for Sn−Ag solders with near eutectic composition (approximately Sn−3.5Ag) [27]. Nevertheless, the microstructure of the as-cast Sn−3.5Ag solder exhibited a hypoeutectic microstructure with *β*-Sn phase as the dominant phase. The hypoeutecticity was attributable to the rapid cooling during the solder fabrication, consistent with Refs. [23,28] in which the rapid cooling led to the formation of finely distributed Ag_3Sn (i.e. eutectic Ag_3Sn). Meanwhile, the microstructures of the as-cast 4.0Ag and 5.0Ag solders that are of hypereutectic composition, were of large plate-like Ag_3Sn phase (primary Ag_3Sn) [29].

Table 2 lists the EDS chemical composition of fine and large plate-like Ag_3Sn in the as-cast 3.0Ag, 3.5Ag, 4.0Ag, and 5.0Ag solders. The EDS results indicated that the contents of Ag in fine (eutectic) and large plate-like

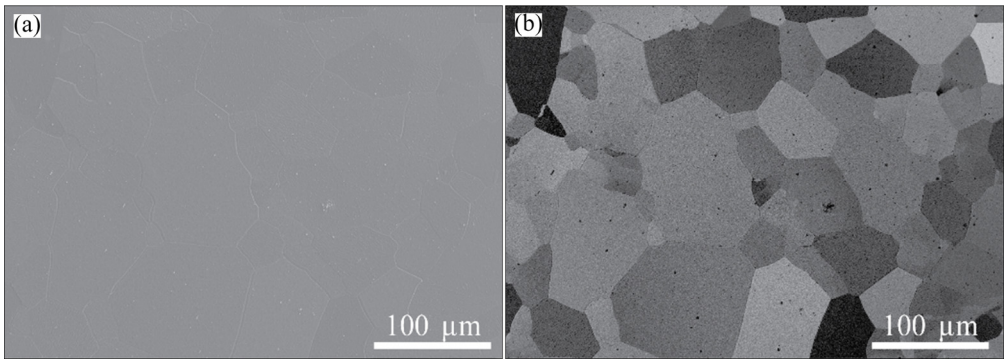

Fig. 1 Microstructures of ion-milled polishing pure Sn (0Ag solder): (a) SEM; (b) BSE-SEM

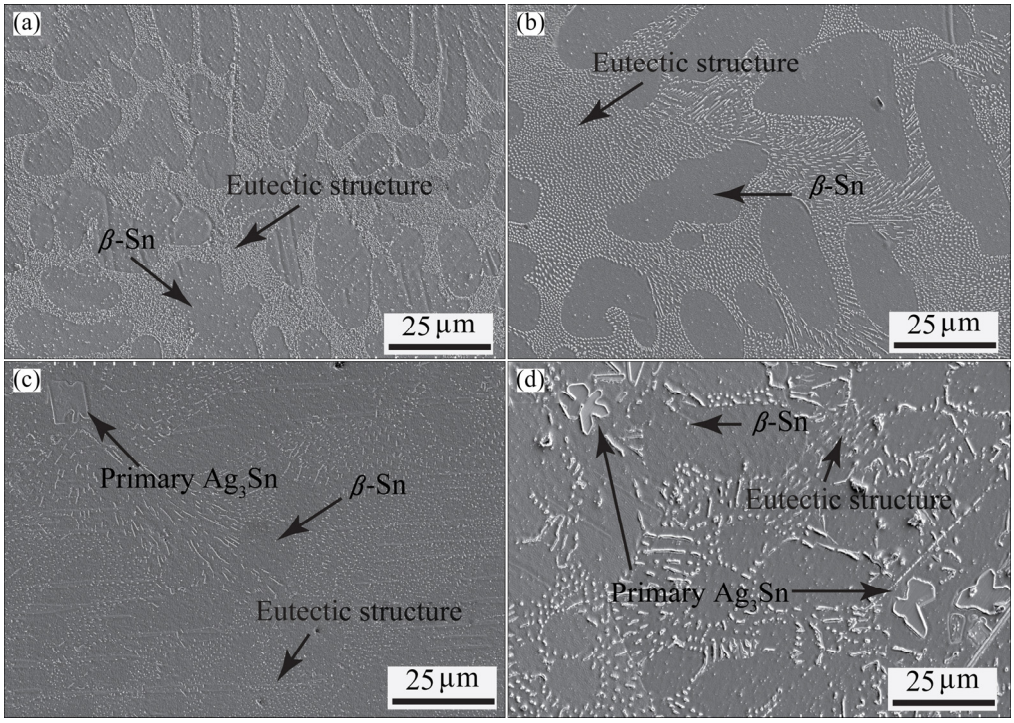

Fig. 2 SEM microstructures of as-cast solders: (a) 3.0Ag; (b) 3.5Ag; (c) 4.0Ag; (d) 5.0Ag

Table 2 Chemical composition of eutectic and primary Ag_3Sn in as-cast 3.0Ag, 3.5Ag, 4.0Ag and 5.0Ag solders (wt.%)

Solder	Eutectic Ag_3Sn		Primary Ag_3Sn	
	Sn	Ag	Sn	Ag
3.0Ag	36.75	63.25	−	−
3.5Ag	33.30	66.70	−	−
4.0Ag	33.58	66.42	36.03	63.97
5.0Ag	29.32	70.68	28.67	70.38

(primary) Ag_3Sn were 63.25−70.68 wt.% and 63.97−70.38 wt.%, respectively, with Sn accounting for the rest. The EDS analysis revealed a close resemblance between the chemical compositions of eutectic and primary Ag_3Sn.

The area fractions of eutectic and primary Ag_3Sn of the 3.0Ag, 3.5Ag, 4.0Ag, and 5.0Ag solders, using ImageJ image processing software, were (10.8±2.6)%, (9.4±0.8)%, (7.8±1.7)%, and (18.3±0.1)%, respectively. Specifically, the elevated Ag content (5.0Ag solder) contributed to the considerably large fraction of Ag_3Sn phase, consistent with Ref. [29], who reported that the large fraction of Ag_3Sn was due to the formation of primary Ag_3Sn which is normally present in Sn−Ag solders with hypereutectic composition. Given that Ag_3Sn is hard and brittle, with the elastic modulus (E) of 90 GPa compared with that of β-Sn phase of 52−68 GPa [6], the Ag content in Sn−xAg solders should thus be taken into account to mitigate the formation of coarse microstructure attributable to the presence of plate-like Ag_3Sn, which in turn adversely alters on the mechanical properties of the solders [29−31].

3.2 Corrosion behavior of as-cast Sn−xAg solders

Figure 3 illustrates the representative potentiodynamic polarization curves of as-cast 0Ag, 3.0Ag, 3.5Ag, 4.0Ag, and 5.0Ag solders in 3.5 wt.% NaCl solution. The corrosion behaviors of the solders were similar, consisting of a cathodic and anodic reaction. Table 3 lists the corrosion parameters, including current density (J_{corr}), corrosion potential (φ_{corr}), anodic Tafel constant (b_a) and cathodic Tafel constant (b_c) of the as-cast Sn−xAg solders in 3.5 wt.% NaCl solution, derived from Tafel fitting of the polarization curves, polarization resistance (R_p) and the corrosion rate (mm/a), determined in accordance with ASTM G3−89 (2010) and G102−89 (2015) standard [32,33]. Polarization resistances (R_p) of the experimental solders, which are inversely correlated with the rate of corrosion, were insignificantly different, varying between 8.72 and 12.42 kΩ. By comparison, however, R_p of the Ag-doped solders (3.0Ag, 3.5Ag, 4.0Ag, and 5.0Ag) was higher than that of the non-Ag solder (0Ag solder), indicating higher corrosion resistance due to the presence of Ag in Sn solders. In other words, the corrosion rate decreased as Ag content increased. Lower corrosion rate in the Ag-doped solders could be attributed to the presence of Ag_3Sn phase which is more thermodynamically stable than Sn-rich phase [10,12]. However, the 5.0Ag solder exhibited higher corrosion rate, probably due to the presence of the large Ag_3Sn fraction, leading to galvanic corrosion and selective oxidation mechanism [12,34]. The galvanic corrosion occurred between the Ag_3Sn and β-Sn phases and selective oxidation of Sn took place in the Ag_3Sn phase. In addition, similarly to R_p, φ_{corr} was positively shifted as the Ag content increased, suggesting a delayed transition from cathodic to anodic reaction. The cathodic reaction associated with all experimental solders commenced at the corrosion potential of −1.2 V and ended at about −0.7 V. Specifically, in the cathodic reaction, the oxidation and hydrogen evolution reactions were the dominant reactions [11,13]. In the anodic reaction, a passivation was observed with the passivation potential (φ_p) between −0.706 and −0.68 V (Table 3), followed by a rapid increase in J_{corr}, resulting in the breakdown of passive film and pitting corrosion [3,14].

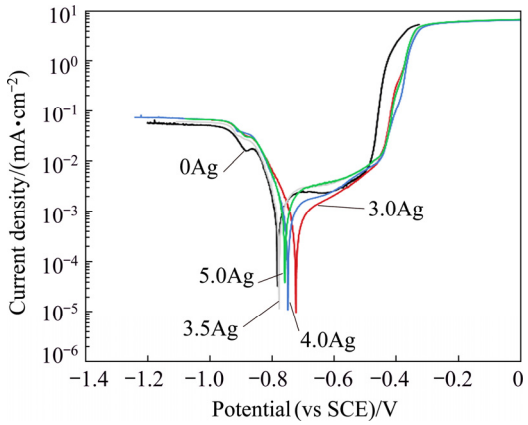

Fig. 3 Representative potentiodynamic polarization curves of as-cast 0Ag, 3.0Ag, 3.5Ag, 4.0Ag and 5.0Ag solders in 3.5 wt.% NaCl solution

Figures 4(a−e) respectively depict the SEM images of corrosion products on the surface of as-cast 0Ag, 3.0Ag, 3.5Ag, 4.0Ag, and 5.0Ag solders. The corrosion products exhibited a similar morphology in which a mixture of platelet-like and needle-like structures with random orientation was observed on the solder surface, consistent with Refs. [2,3,11,14]. Figure 5 depicts the cracking of passive film and pitting corrosion observed on the surface of all experimental solders. Table 4 lists the EDS chemical composition of the corrosion products on the surface of Sn−xAg solders, given variable Ag contents (0, 3.0, 3.5, 4.0, 5.0 wt.%). The corrosion products were mainly Sn, Cl, and O, with relatively small amounts of Ag. Given the presence of Cl and O,

Table 3 Parameters of corrosion behavior of as-cast Sn−*x*Ag solders in 3.5 wt.% NaCl solution

Solder	J_{corr}/(μA·cm^{-2})	φ_{corr}/V	b_a/(mV·dec^{-1})	b_c/(mV·dec^{-1})	φ_p/V	R_p/kΩ	Corrosion rate/(mm·a^{-1})
0Ag	4.61±0.3	−0.758±0.02	454±12.0	119±23.3	−0.704±0.003	8.72±0.8	0.1227±0.001
3.0Ag	3.65±0.06	−0.739±0.01	459±23.2	127±10.5	−0.680±0.008	12.42±0.8	0.0983±0.001
3.5Ag	3.06±0.1	−0.771±0.005	840±10.7	85±7.0	−0.702±0.004	11.15±0.3	0.0815±0.004
4.0Ag	3.92±0.5	−0.749±0.001	748±6.4	119±5.4	−0.686±0.002	10.42±1.1	0.1151±0.100
5.0Ag	4.09±0.8	−0.754±0.006	782±13.5	121±1.2	−0.683±0.007	10.42±2.6	0.125±0.026

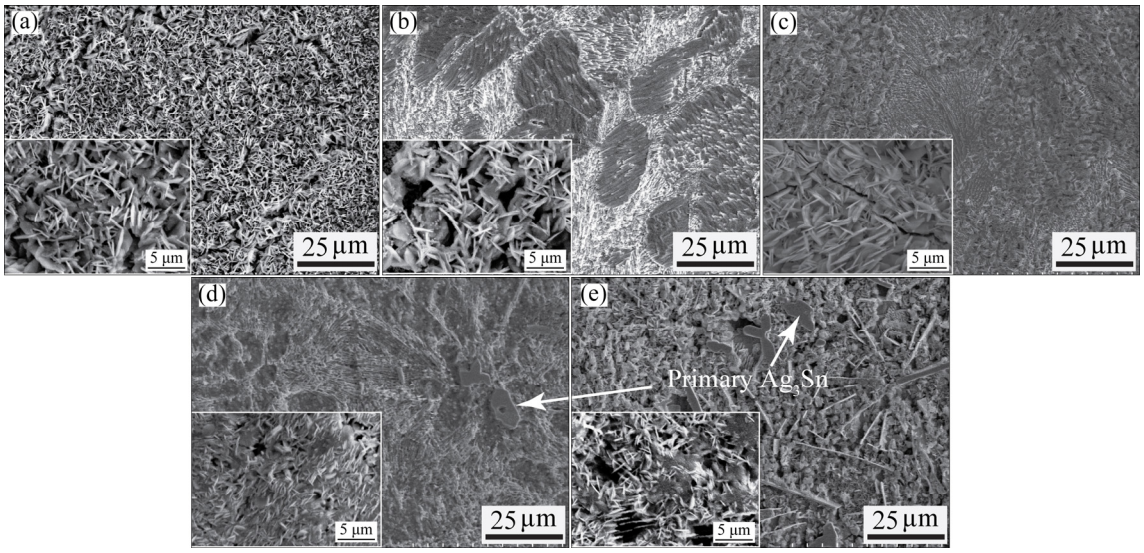

Fig. 4 SEM images of corrosion products on surface of as-cast solders: (a) 0Ag; (b) 3.0Ag; (c) 3.5Ag; (d) 4.0Ag; (e) 5.0Ag

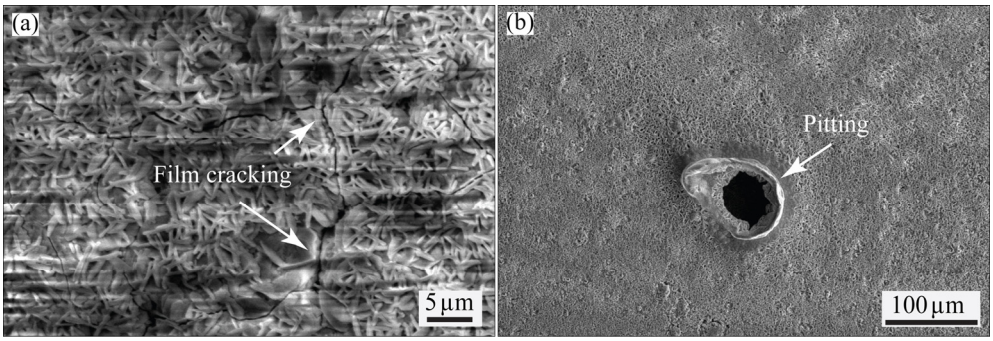

Fig. 5 Representative images of film cracking (a) and pitting corrosion (b)

Sn reacted with Cl and O to form tin-oxide chloride hydroxide ($Sn_3O(OH)_2Cl_2$) [11,13], which could be expressed as

$$3Sn+4OH^-−6e+2Cl^-=Sn_3O(OH)_2Cl_2+H_2O \quad (1)$$

The presence of Ag in the corrosion product (Table 4) was attributable to selective oxidation as a result of the lower Gibbs free energy of SnO_2 (−515.8 kJ/mol) relative to that of Ag_2O (−11.2 kJ/mol) [12,34,35]. Specifically, due to the lower Gibbs free energy, the oxidation of Sn in the eutectic and primary Ag_3Sn phases preceded that of Ag, which could be expressed as

$$Ag_3Sn+O_2 \rightarrow SnO_2+3Ag \quad (2)$$

$$2Ag_3Sn+O_2 \rightarrow 2SnO_2+6Ag \quad (3)$$

Table 4 Chemical composition of corrosion products on surface of experimental solders

Solder	Content/wt.%			
	Sn	Ag	Cl	O
0Ag	35.76	−	29.49	34.75
3.0Ag	39.74	0.30	26.58	33.37
3.5Ag	33.25	5.02	24.82	36.91
4.0Ag	35.07	0.38	30.43	34.12
5.0Ag	34.05	2.91	25.73	37.32

3.3 Effect of Ag on formation of intermetallic layer

Figure 6 compares the wettability of the experimental solders as a function of spreading factor. The average spreading factors of the 0Ag, 3.0Ag, 3.5Ag,

4.0Ag, and 5.0Ag solders on Cu substrate were 94.5%, 94.6%, 93.08%, 94.2%, and 95.06%, respectively. The insignificant difference among the spreading factors indicated that Ag had negligible effects on the wettability of Sn−*x*Ag solders on Cu substrate.

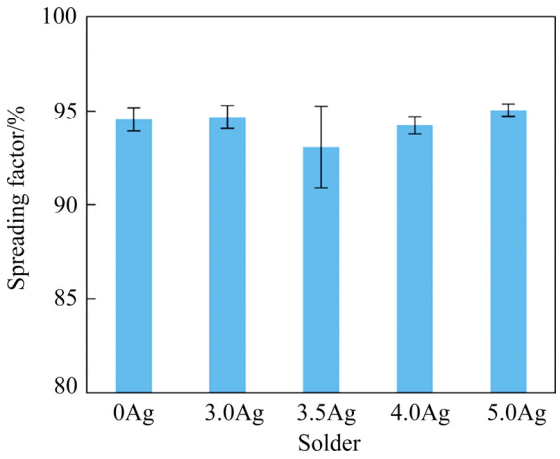

Fig. 6 Spreading factor of 0Ag, 3.0Ag, 3.5Ag, 4.0Ag and 5.0Ag solders on Cu substrate

Figures 7(a)−(e) respectively illustrate the morphologies of the intermetallic layer of the 0Ag, 3.0Ag, 3.5Ag, 4.0Ag, and 5.0Ag solders with Cu substrate. A scallop-shaped intermetallic layer, consisting of Sn and Cu, was observed at the interfacial layer between the solders and Cu substrate. The microstructures of the pre- and post-soldering solders were in good agreement, whereby no Ag_3Sn was present in the 0Ag solder joint and the finely distributed Ag_3Sn (eutectic Ag_3Sn) was observed in the 3.0Ag and 3.5Ag joints. Besides, the primary Ag_3Sn (large plate-like Ag_3Sn) and eutectic Ag_3Sn were formed in the 4.0Ag and 5.0Ag joints. The compositions of Cu and Sn were approximately 56 wt.% and 39 wt.% for all the experimental solders, indicating the formation of Cu_6Sn_5, which could be expressed as

$$6Cu+5Sn\longrightarrow Cu_6Sn_5 \quad (4)$$

In the experiment, no Cu_3Sn phase was detected at the interface. The absence of Cu_3Sn phase was probably attributed to the short soldering time, consistent with Ref. [4]. In addition, from the thermodynamic viewpoint, the activation energy of the formation of Cu_3Sn phase is considerably higher than that of Cu_6Sn_5 phase [4,26,36], giving rise to the formation of Cu_6Sn_5 during soldering, as expressed in Eq. (4).

Figure 8 illustrates the cross-sectional EDS map analyses of the 3.5Ag and 5.0Ag solder joints. Specifically, the 3.5Ag solder joint contained only the finely distributed Ag_3Sn (eutectic Ag_3Sn), while both the eutectic and primary Ag_3Sn phases were present in the 5.0Ag solder joint. By comparison, Ag_3Sn was more prevalent than Cu_6Sn_5 in the solder matrix.

Figure 9 compares the intermetallic-layer thickness of the 0Ag, 3.0Ag, 3.5Ag, 4.0Ag, and 5.0Ag solders, with the respective thicknesses of 2.05, 1.14, 1.58, 1.78, and 1.86 μm. By comparison, the intermetallic layer of the Ag-doped solders was thinner than that of the non-Ag solder (0Ag solder). The smaller thickness was attributable to the presence of finely distributed (eutectic) and large plate-like (primary) Ag_3Sn in the Ag-doped solders (Figs. 7 and 8). Specifically, the fine Ag_3Sn particles (eutectic Ag_3Sn) precipitating on the surface of solidified and grain boundaries of Cu_6Sn_5 impeded the growth of Cu_6Sn_5 grains. In addition, the fine Ag_3Sn particles pinned the diffusion channels, preventing Cu atoms diffusing from the Cu substrate and subsequently hindering the formation of Cu_6Sn_5 [37]. The phenomenon is referred to as the shielding effect of Ag_3Sn on the growth of Cu_6Sn_5 grains [22,38,39].

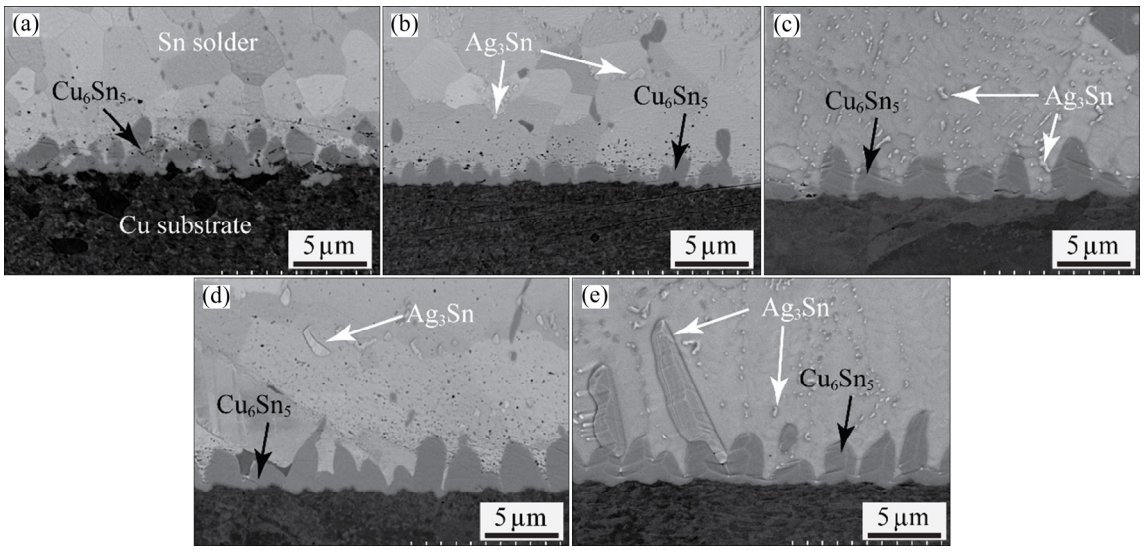

Fig. 7 Morphologies of intermetallic layer of 0Ag (a), 3.0Ag (b), 3.5Ag (c), 4.0Ag (d), 5.0Ag (e) solders with Cu substrate

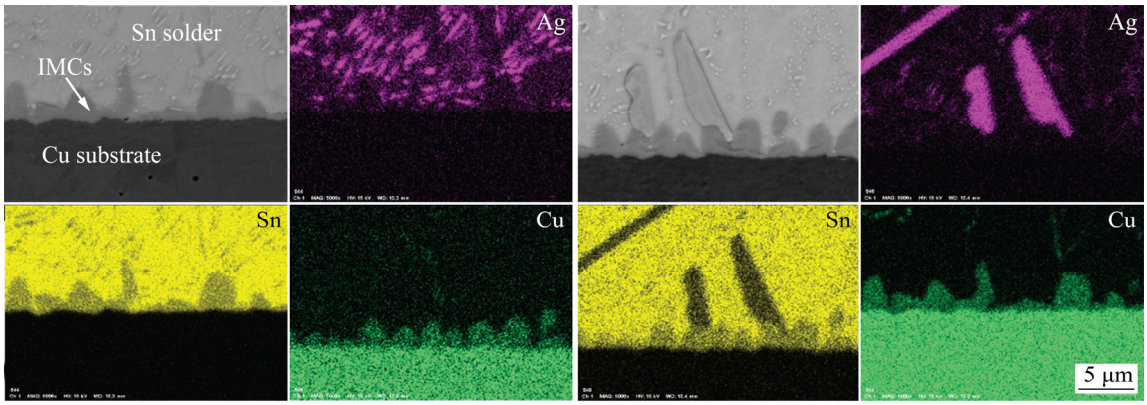

Fig. 8 Cross-sectional EDS map analysis of 3.5Ag (a) and 5.0Ag (b) solder joints

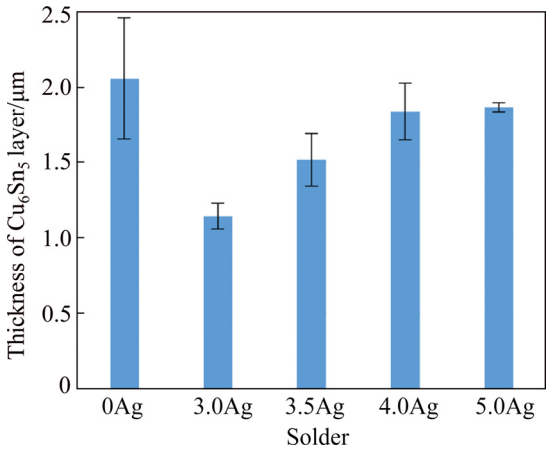

Fig. 9 Thickness of intermetallic layer (Cu_6Sn_5) of experimental solders

However, the shielding effect was restricted by the presence of large plate-like Ag_3Sn with increase in the Ag content (i.e. 4.0Ag and 5.0Ag solders), resulting in the increased thickness of the intermetallic layer.

Moreover, the competitive growth between Cu_6Sn_5 and Ag_3Sn phases during soldering influenced the shielding effect of Ag_3Sn [37]. Based on the activation energy, the formation of Ag_3Sn requires less energy than that of Cu_6Sn_5 [40,41], contributing to the prevalence of Ag_3Sn with finer and more uniformly distributed microstructure. The ubiquity of fine (eutectic) Ag_3Sn is advantageous to the improved reliability of Sn–*x*Ag solder system and Sn–*x*Ag/Cu joints as well as the enhanced corrosion resistance. In contrast, the presence of large plate-like (primary) Ag_3Sn accelerates the failure of Sn–*x*Ag/Cu joints [29]. Specifically, the tensile and shear strengths of the joints decrease due to the brittleness of Ag_3Sn, which in turn adversely affects the durability and reliability of solder joints [4,29]. To mitigate the formation of large plate-like Ag_3Sn phase, the Ag content in Sn–Ag solders should thus be of hypoeutectic composition between 3.0 and 3.5 wt.%.

4 Conclusions

(1) The morphology of Ag_3Sn phase evolved from the fine particles to large plate-like crystals as the Ag content increased. Specifically, in the 3.0Ag and 3.5Ag solders, β-Sn phase was surrounded by eutectic networks, and large plate-like Ag_3Sn was formed in the 4.0Ag and 5.0Ag solders. In addition, the elevated Ag content contributed to the considerably large fraction of Ag_3Sn phase.

(2) The Ag content slightly affected the corrosion behavior of the as-cast Sn–*x*Ag solders. In addition, the transition from a cathodic to anodic reaction was delayed after the introduction of Ag into Sn–*x*Ag solders resulting in the decreasing of the corrosion rate.

(3) The analysis of the intermetallic layer of the 3.0Ag and 3.5Ag solders revealed the shielding effect of Ag_3Sn on the growth of Cu_6Sn_5 grains, whereby the fine Ag_3Sn particles in the eutectic networks precipitating on the surface of Cu_6Sn_5 obstructed the development of Cu_6Sn_5 grains, and pinned the diffusion channels preventing Cu atoms diffusing from the Cu substrate. However, the shielding effect was blunted by the presence of large plate-like Ag_3Sn in the 4.0Ag and 5.0Ag solders, resulting in the increased thickness of the intermetallic layer.

Acknowledgements

The authors gratefully acknowledge Ms. Sukanya Unarat for her assistance with metallographic specimen preparation for SEM observation. The authors also would like to thank Ms. Suwattana Thongkarm and Mr. Sakul Chotthanasak of Coax group Corporation Ltd., Thailand, for contributing to ion-milling polishing and the SEM analysis. Thanks also to the Center for Advanced Studies in Nanotechnology for Chemical, Food and Agricultural Industries, Kasetsart University

Insititute of Advanced Studies (KUIAS) for valuable help in the EDS analysis.

References

[1] YANG Fan, ZHANG Liang, LIU Zhi-quan, ZHONG Su-juan, MA Jia, BAO Li. Properties and microstructures of Sn−Bi−X lead-free solders [J]. Advances in Materials Science and Engineering, 2016, 2016: 1−15.

[2] MOHANTY U S, LIN K L. Electrochemical corrosion behaviour of lead-free Sn−8.5Zn−*X*Ag−0.1Al−0.5Ga solder in 3.5% NaCl solution [J]. Materials Science and Engineering A, 2005, 406: 34−42.

[3] LIU J C, PARK S W, NAGAO S, NOGI M, KOKA H, MA J S, ZHANG G, SUGANUMA K. The role of Zn precipitates and Cl^- anions in pitting corrosion of Sn−Zn solder alloys [J]. Corrosion Science, 2015, 92: 263−271.

[4] LEE L M, MOHAMAD A A. Interfacial reaction of Sn−Ag−Cu lead-free solder alloy on Cu: A review [J]. Advances in Materials Science and Engineering, 2013, 2013: 1−11.

[5] AMAGAI M. A study of nanoparticles in Sn−Ag based lead free solders [J]. Microelectronics Reliability, 2008, 48: 1−16.

[6] LOTFIAN S, MOLINA-ALDAREGUIA J M, YAZZIE K E, LLORCA J, CHAWLA N. Mechanical characterization of lead-free Sn−Ag−Cu solder joints by high-temperature nanoindentation [J]. Journal of Electronic Materials, 2013, 42: 1085−1091.

[7] KOTADIA HIREN R, HOWES PHILIP D, MANNAN S. A review: On the development of low melting temperature Pb-free solders [J]. Microelectronics Reliability, 2014, 54: 1253−1273.

[8] SHEN J, LIU Y C, GAO H X, WEI C, YANG Y Q. Formation of bulk Ag_3Sn intermetallic compounds in Sn−Ag lead-free solders in solidification [J]. Journal of Electronic Materials, 2005, 34: 1591−1597.

[9] KANLAYASIRI K, ARIGA T. Physical properties of Sn58Bi−*x*Ni lead-free solder and its interfacial reaction with copper substrate [J]. Materials and Design, 2015, 86: 371−378.

[10] OSÓRIO W R, PEIXOTO L C, GARCIA L R, GARCIA A, SPINELLI J. The effects of microstructure and Ag_3Sn and Cu_6Sn_5 intermetallics on the electrochemical behavior of Sn−Ag and Sn−Cu solder alloys [J]. International Journal of Electrochemical Science 2012, 7: 6436−6452.

[11] LI D Z, CONWAY P P, LIU C Q. Corrosion characterization of tin-lead and lead free solders in 3.5 wt.% NaCl solution [J]. Corrosion Science, 2008, 50: 995−1004.

[12] WANG M, WANG J Q, FENG H, KE W. Effect of Ag_3Sn intermetallic compounds on corrosion of Sn−3.0Ag−0.5Cu solder under high-temperature and high-humidity condition [J]. Corrosion Science, 2012, 63: 20−28.

[13] GAO Yan-fang, CHENG Cong-qian, ZHAO Jie, WANG Li-hua, LI Xiao-gang. Electrochemical corrosion of Sn−0.75Cu solder joints in NaCl solution [J]. Transactions of Nonferrous Metals Society of China, 2012, 22: 977−982.

[14] BUI Q V, NAM N D, NOH B I, KAR A, KIM J G, JUNG S B. Effect of Ag addition on the corrosion properties of Sn-based solder alloys [J]. Materials and Corrosion, 2010, 61: 30−33.

[15] FAYEKA M, FAZAL M A, HASEEB A S M A. Effect of aluminum addition on the electrochemical corrosion behavior of Sn−3Ag−0.5Cu solder alloy in 3.5 wt% NaCl solution [J]. Journal of Materials Science: Materials in Electronics, 2016, 27: 12193−12200.

[16] ZHANG Liang, XUE Song-bai, GAO Li-li, DAI Wei, JI Feng, CHEN Yan, YU Sheng-lin, Microstructure characterization of SnAgCu solder bearing Ce for electronic packaging [J]. Microelectronic Engineering, 2011, 88: 2848−2851.

[17] SHEN Jun, PU Ya-yun, YIN Heng-gang, TANG Qin. Effects of Cu, Zn on the wettability and shear mechanical properties of Sn−Bi-based lead-free solders [J]. Journal of Electronic Materials, 2015, 44: 532−541.

[18] MA Dong-liang, WU Ping. Effects of Zn addition on mechanical properties of eutectic Sn-58Bi solder during liquid-state aging [J]. Transactions of Nonferrous Metals Society of China, 2015, 25: 1225−1233.

[19] KLASIK A, SOBCZAK N, MAKOWSKA K, WOJCIECHOWSKI A, KUDYBA A, SIENICKI E K. Relationship between mechanical properties of lead-free solders and their heat treatment parameters [J]. Journal of Materials Engineering and Performance, 2012, 21: 620−628.

[20] LAURILA T, HURTIG J, VUORINEN V, KIVILAHTI J K. Effect of Ag, Fe, Au and Ni on the growth kinetics of Sn−Cu intermetallic compound layers [J]. Microelectronics Reliability, 2009, 49: 242−247.

[21] LAURILA T, VUORINEN V, PAULASTO-KRÖCKEL M. Impurity and alloying effects on interfacial reaction layers in Pb-free soldering [J]. Materials Science and Engineering R: Reports, 2010, 68: 1−38.

[22] GUO Bing-feng, KUNWAR A, ZHAO Ning, CHEN Jun, WANG Yun-peng, MA Hai-tao. Effect of Ag_3Sn nanoparticles and temperature on Cu_6Sn_5 IMC growth in Sn−*x*Ag/Cu solder joints [J]. Materials Research Bulletin, 2018, 99: 239−248.

[23] LEE H T, CHEN Yin-fa. Evolution of Ag_3Sn intermetallic compounds during solidification of eutectic Sn−3.5Ag solder [J]. Journal of Alloys and Compounds, 2011, 509: 2510−2517.

[24] LIN D C, SRIVATSAN T S, WANG G X, KOVACEVIC R. Microstructural development in a rapidly cooled eutectic Sn−3.5% Ag solder reinforced with copper powder [J]. Powder Technology, 2006, 166: 38−46.

[25] SEO S K, KANG S K, SHIH D Y, LEE H M. An investigation of microstructure and microhardness of Sn−Cu and Sn−Ag solders as functions of alloy composition and cooling rate [J]. Journal of Electronic Materials, 2009, 38: 257−265.

[26] KANLAYASIRI K, SUKPIMAI K. Effects of indium on the intermetallic layer between low-Ag SAC0307-*x*In lead-free solders and Cu substrate [J]. Journal of Alloys and Compounds, 2016, 668: 169−175.

[27] OH C S, SHIM J H, LEE B, LEE D N. A thermodynamic study on the Ag−Sb−Sn system [J]. Journal of Alloys and Compounds, 1996, 238: 155−166.

[28] OCHOA F, WILLIAMS J J, CHAWLA N. Effects of cooling rate on the microstructure and tensile behavior of a Sn−3.5wt.%Ag solder [J]. Journal of Electronic Materials, 2003, 32: 1414−1420.

[29] KIM K S, HUH S H, SUKANUMA K. Effects of intermetallic compounds on properties of Sn−Ag−Cu lead-free soldered joints [J]. Journal of Alloys and Compounds, 2003, 352: 226−236.

[30] FOUASSIER O, HEINTZ J M, CHAZELAS J, GEFFROY P M, SILVAIN J F. Microstructural evolution and mechanical properties of SnAgCu alloys [J]. Journal of Applied Physics, 2006, 100: 043519-1–7.

[31] HUH S H, KIM K S, SUKANUMA K. Effect of Ag addition on the microstructural and mechanical properties of Sn−Cu eutectic solder [J]. Materials Transactions, 2001, 42: 739−744.

[32] ASTM G3-89(2010). Standard practice for conventions applicable to electrochemical measurements in corrosion testing [S]. West Conshohocken, PA: ASTM International, 2010.

[33] ASTM G102-89(2015)e1. Standard practice for calculation of corrosion rates and related information from electrochemical measurements [S]. West Conshohocken, PA: ASTM International, 2015.

[34] WANG Ming-na, WANG Jian-qiu, KE Wei. Effect of microstructure and Ag_3Sn intermetallic compounds on corrosion behavior of

Sn−3.0Ag−0.5Cu lead-free solder [J]. Journal of Materials Science: Materials in Electronics, 2014, 25: 5269−5276.

[35] DUDEK M A, CHAWLA N. Oxidation behavior of rare-earth-containing Pb-free solders [J]. Journal of Electronic Materials, 2009, 38: 210−220.

[36] YOON J W, LEE C B, KIM D U, JUNG S B. Reaction diffusions of Cu_6Sn_5 and Cu_3Sn intermetallic compound in the couple of Sn−3.5Ag eutectic solder and copper substrate [J]. Metals and Materials International, 2003, 9: 193−199.

[37] YU D Q, WANG L, WU C M L, LAW C M T. The formation of nano-Ag_3Sn particles on the intermetallic compounds during wetting reaction [J]. Journal of Alloys and Compounds, 2005, 389: 153−158.

[38] YU S P, WANG M C, HON M H. Formation of intermetallic compounds at eutectic Sn−Zn−Al solder/Cu interface [J]. Journal of Materials Research, 2001, 16: 76−82.

[39] YANG Ming, LI Ming-yu, WANG Chun-qing. Interfacial reactions of eutectic Sn3.5Ag and pure tin solders with Cu substrates during liquid-state soldering [J]. Intermetallics, 2012, 25: 86−94.

[40] SU T L, TSAO L C, CHANG S Y, CHUANG T H. Morphology and growth kinetics of Ag_3Sn during soldering reaction between liquid Sn and an Ag substrate [J]. Journal of Materials Engineering and Performance, 2002, 11: 365−368.

[41] SHAO Hua-kai, WU Ai-ping, BAO Yu-dian, ZHAO Yue, ZOU Gui-sheng. Mechanism of Ag_3Sn grain growth in Ag/Sn transient liquid phase soldering [J]. Transactions of Nonferrous Metals Society of China, 2017, 27: 722−732.

Sn–*x*Ag 无铅焊料中 Ag 含量对其显微组织、腐蚀行为和与 Cu 基体界面反应的影响

Phacharaphon TUNTHAWIROON, Kannachai KANLAYASIRI

Department of Industrial Engineering, Faculty of Engineering,
King Mongkut's Institute of Technology Ladkrabang, Bangkok 10520, Thailand

摘　要：研究不同 Ag 含量(0、3.0%、3.5%、4.0%和 5.0%，质量分数)对预焊 Sn−*x*Ag 无铅焊料显微组织和腐蚀行为的影响，以及对焊料与铜基体间形成金属间化合物界面层的影响。Ag 含量对焊料中 Ag_3Sn 相的形貌有一定的影响。显微组织分析结果表明，在 3.0Ag 和 3.5Ag 焊料中，β-Sn 相被共晶组织网络所包围；在 4.0Ag 和 5.0Ag 焊料中，形成大的片状 Ag_3Sn 相。但是，动电位极化曲线测试结果显示，Ag 含量对铸态焊料腐蚀行为的影响甚微。与铜基体焊接后，在 Sn–*x*Ag/Cu 界面处仅形成单层的 Cu_6Sn_5 金属间化合物。与未掺 Ag 的焊料相比，掺 Ag 的焊料与基体的界面中形成的 Cu_6Sn_5 金属间化合物层更薄。与 4.0 Ag 和 5.0Ag 焊料中形成的大片状 Ag_3Sn 相比，在 3.0Ag 和 3.5Ag 焊料中析出的共晶网络中细小的 Ag_3Sn 颗粒沉淀，能更有效地抑制 Cu_6Sn_5 晶粒的生长。

关键词：Sn−Ag 无铅焊料；显微组织；Ag_3Sn 金属间化合物相；腐蚀行为；Cu_6Sn_5 金属间化合物层；润湿性

(Edited by Xiang-qun LI)